REX2024
PRCI Research Exchange

Effect of water vapor and H_2S on the hydrogen embrittlement sensitivity of underground gas storage carbon steels assets

Presented at the

Pipeline Research Council International

2024 Research Exchange

Authors:

Clara JUILLET[(1)], Xavier CAMPAIGNOLLE[(1)], Christophe POMMIER[(2)],

Lisa BLANCHARD[(3)], Laurent BRIOTTET[(3)]

[(1)]STORENGY SAS, 12 rue Raoul Nordling CS 50014, 92277 Bois-Colombes Cedex, France

[(2)]STORENGY FRANCE, 12 rue Raoul Nordling CS 70001, 92274 Bois-Colombes Cedex, France

[(3)]Univ. Grenoble Alpes, CEA LITEN, DTCH, LCA, F-38000 Grenoble, France

Abstract

Storengy is a European leader in the design, construction, operation, and maintenance of natural gas underground storage (UGS) assets (salt caverns and porous reservoirs: aquifers and depleted fields). In France, Storengy currently operates 14 sites of natural gas (NG) UGS. Storengy foresees to become a key actor in the new energy transition markets and is therefore involved in new activities to convert existing UGS assets and develop new ones for renewable gases (biomethanes, e-methanes, H_2 blended or/and pure).

Hydrogen offers promising potential for a sustainable energy transition and to eventually achieve carbon neutrality. The growing need for gaseous hydrogen as an energy carrier requires the development of specific gas infrastructures. In particular, large quantities of hydrogen will be stored in underground salt caverns, as it is already the case for natural gas. In addition, hydrogen will be present in new methanes, such as those from pyro-gasification, and therefore blended H_2 will be present in the existing natural gas infrastructures. In underground storages, both porous media or salt caverns, liquid water (or brine) is in contact with the gas. Consequently, the water vapor content of the withdrawn gas is higher than the injected one coming from the transmission network. It may even reach saturation. As a matter of fact, all UGS are equipped with dehydration units. In addition, under specific conditions (i.e. specific storages), souring (H_2S production) may be observed, and desulfuration units are implemented.

The hydrogen injection, either pure or blended with natural gas, into various equipment exposes the materials in contact with the injected gas to the risks of hydrogen embrittlement. Hydrogen embrittlement is a physical phenomenon that degrades some mechanical properties (ductility, toughness…) and promotes crack initiation and growth. The literature is lacking data on the effect of water vapor and low H_2S levels on hydrogen embrittlement susceptibility to of steels used in UGS infrastructures. Nevertheless, the literature has highlighted impacts of some gas impurities on the hydrogen embrittlement of steels. Indeed, oxygen is reported to inhibit hydrogen embrittlement, whereas H_2S would act as a catalyst.

This work investigates mechanical properties of a tempered martensite N80Q steel, and a ferrite-perlite L360 C Mn steel issued from a completion tubing and a flowline pipeline respectively, both coming from the field. The testing environments are NG + 25%H_2 and NG saturated with water vapor with and without H_2S (30 mg/Nm^3) at 85 bar and room temperature. Regarding toughness tests, although the two steels showed acceptable values (regarding ASME), they presented different behaviors. For L360, only the NG + 25%H_2 + H_2O + H_2S environment generated crack propagation, indicating a synergetic effect between H_2 and H_2S. On the contrary, cracks propagated in all N80Q tests, showing no influence of H_2 and H_2S. Based on the literature C-Mn steels toughness is affected by the presence of dry hydrogen. Hence, the results presented here show that H_2O inhibits hydrogen embrittlement as far as toughness is concerned.

However, the FCGR (Fatigue Crack Growth Rate) results clearly demonstrated the influence of hydrogen on the mechanical behavior of both steels. FCGR are faster by a factor of five (resp. 10) in NG + 25%H_2 + H_2O than in NG + H_2O for N80Q (resp. L360).

The aim of this presentation is to demonstrate the importance of mechanically testing materials in

specific hydrogenated environment with contents of H_2O and H_2S representative of field conditions. These results will be used to assess the compatibility of existing storage facilities steels to H_2 service, either pure or blended; and to choose fitting for purpose materials for new (or upgraded) facilities.

Table of Contents

List of Figures

List of Acronyms

a Specimen crack length

COD Clip-on displacement

CTOD Crack tip opening displacement

Fnorm Normalised load

FCG Fatigue Crack Growth

FCGR Fatigue Crack Growth Rate

FT Fracture Toughness

HE Hydrogen embrittlement

P_{tot} Total pressure of the test

RH Relative humidity

RT Room temperature

SSC Sulfide stress cracking

ΔK Stress intensity factor amplitude

$\Delta K_{th,H2}$ Stress intensity factor amplitude above which hydrogen influence is observed

1 Executive Summary

A key point for the development of a renewable energy economy at a large scale is the possibility to use the current natural gas network and storage capacity to transport and store hydrogen. This study is dedicated to evaluate the integrity of materials used for underground aquifer storage regarding hydrogen embrittlement in a gaseous environment saturated with water vapor and containing some H_2S. In this environment, the stored gas water vapor content may reach saturation at bottom well pressure and temperature. It is known that the presence of impurities in the gas, such as H_2O, O2 or H2S, may promote or inhibit hydrogen embrittlement phenomenon, depending on the steel grade. This work investigates mechanical properties of a tempered martensite N80-Q steel, and a ferrite-perlite L360-NB C-Mn steel issued from a completion and a collect tube respectively. The testing environments are NG, NG + H_2S, NG + 25%H_2 and NG + 25%H_2 + H_2S saturated in water vapor at 8.5 MPa and room temperature. These environmental conditions aim at replicating the storage service conditions. Fracture toughness and fatigue crack growth properties are assessed. So far, the mechanical behavior of such steels under hydrogen gas pressure saturated with water vapor and low amount of H_2S has poorly been addressed. Regarding toughness properties, the two steels present different behaviors : for the L360 NB crack has not propagated for any of the testing environments, while cracks propagated in all the tests for the N80 Q. Despite this difference, for the two steels, the toughness does not seem to be affected by hydrogen as the results obtained in NG + 25%H_2 + H_2O and NG + H_2O are similar. Based on the literature C-Mn steels toughness is affected by the presence of dry hydrogen. Hence, the results presented here show that H_2O inhibits hydrogen embrittlement as far as toughness is concerned. The L360NB, however, presented a slight decrease in toughness properties with the combination of NG + 25%H_2 + H_2S + H_2O. FCG (fatigue crack growth) results, on the opposite, clearly highlight the influence of hydrogen on the mechanical behavior of the two steels. The FCG rates are faster from a factor five (resp. 10) in NG + 25%H_2 + H2O compared to NG + H_2O for the N80 Q (resp. L360). In this article, toughness and FGC results on the two steels are discussed in terms of microstructure and mechanical loading modes, aiming to quantify and better understand the influence of H_2O and H_2S on the sensitivity of low alloy steels to hydrogen embrittlement.

2 Introduction

The European goal of carbon neutrality by 2050 has driven many countries in investing for the deployment of green gases (hydrogen and synthetic methane) as energy carriers and as a mean for decarbonisation of a wide range of industrial sectors [1]. However, a critical element for the development of the renewable gas economy at a large scale is the possibility to use the current natural gas network and storage capacity to transport and store hydrogen (as even synthetic methanes may content some H_2).

Hydrogen storage can be addressed by several means such as physical storage (compressed of liquid hydrogen), adsorption or chemical storage (including chemical hydrides and chemical hydrides) [2], [3]. However, for long-term and large-scale hydrogen storage, geological formations are the best candidates [4-5]. This includes aquifer and depleted gas [6] and oil reservoirs, underground salt caverns [7] and lined-rock caverns [8-9].

In this context, STORENGY is looking at using its underground gas storage capacities for green gas storage, and specifically its aquifer capacities. In these conditions, the gas can get saturated with water vapor and contaminated by small amount of H_2S (i.e. 25 ppmv). The present study aimed to investigate the integrity of a well tubing (L360 NB steel) and a flowline (N80 Q) pipeline steels that would be in contact with such gas.

If the sensitivity to hydrogen embrittlement of low alloy steels in the presence of dry hydrogen is well established [10-12], only few data exist on the influence of water vapor and low amount of H_2S in gaseous hydrogen on promoting or inhibiting hydrogen embrittlement sensitivity, although some studies concerning hydrogen diffusion in brine have been carried out [5]. Figure 1, presents the fatigue crack growth (FCG) and fracture toughness results of several low alloy steels in the presence of H_2S and H_2O separately [13-15]. The enhancement of HE by the presence of relatively high amount of H_2S was observed on the FCG and fracture toughness results. Moreover, the influence of water vapor is dependent on the material : HE sensitivity is increased for the 2.25CrMo and decreased for the AISI 4340.

The literature did not address neither the influence of low amount of H_2S, nor the combination of H_2S+H_2O on HE sensitivity of steels. This work investigates fatigue crack growth and fracture toughness behavior of a tempered martensite N80 Q steel and a ferrite-perlite L360 NB CMn steel issued from a completion and a collect tube respectively, in testing conditions aiming at replicate the storage service conditions.

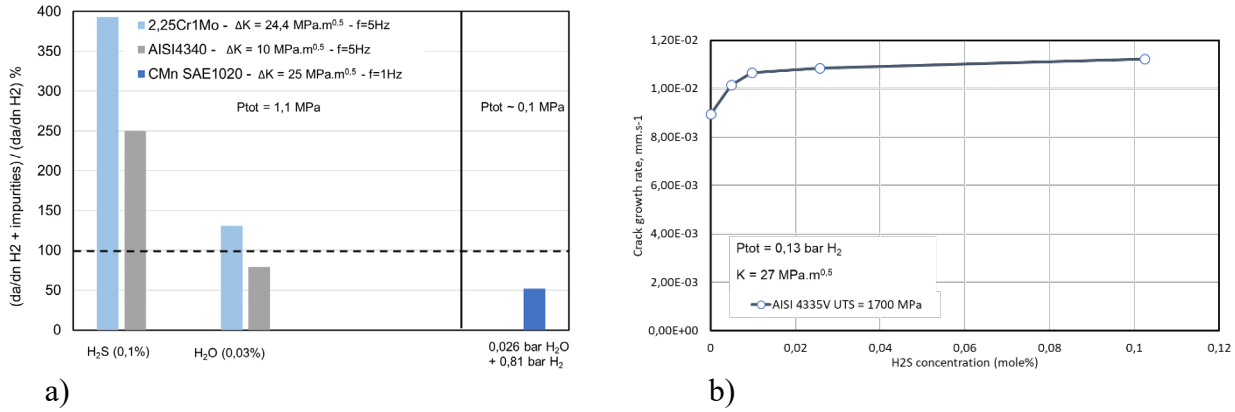

Figure 1: a) Fatigue crack growth data on the influence of H_2S, H_2O and the mixture H_2O+H_2 on a 2.2Cr1Mo, AISI4340 CMn SAE1020 carbon steels [13-15] and b) fracture toughness results on the influence of H_2S on hydrogen embrittlement sensitivity of a AISI4335V.

3 Content

3.1 Experimental Materials and Methods

3.1.1 Materials

Two steels were investigated in this work: a flowline pipe L360 NB seamless (2009), satisfying the ISO 10474 3.1B and a well completion tubing N80 Q (2020) satisfying the API 5CT (quenched

at 925°C for 10 min and 690°C 15 min tempering). Both grades complied with standards for resistance to mild sulphide environments. The results of the L360 NB will be compared with previous results obtained on a seam welded X52 HRR vintage pipeline manufactured in 1969 and satisfying the B121.23 specification. Indeed, the two alloys have close compositions, microstructures and mechanical properties.

3.1.2 Testing environments

The composition of the NG was chosen as close as possible from service condition as the presence of impurities (e.g. N_2, CO_2, H_2S, O_2, THT, etc.) could influence HE sensitivity. The tests were performed at 85 bar and room temperature. The influence of water vapour was investigated by forcing the testing gas through a bubbler ensuring its saturation. The concentration of H_2S in the pressure vessel was ensured by a continuous flow of the testing gas through the pressure vessel. This way, despite the dissolution of H_2S in the bubbler and its adsorption on the set up surfaces, H_2S concentration in the pressure vessel corresponds to the required value. Water saturation of the gas was measured thanks to a gas sampler located after the pressure vessel allowing for testing gas analysis. The H_2S concentration was controlled and measured with a micro gas chromatograph (Micro-GC).

The L360 NB and N80 Q steels were tested in NG, NG + H_2S, NG + 25%H_2 and NG + 25%H_2 + H_2S saturated in water vapour. The results on the X52 HRR were obtained in dry NG, NG +2%H_2, NG+25%H_2 and 100%H_2.

3.1.3 Mechanical testing procedure

3.1.3.1 Specimens geometry

Fatigue crack growth and fracture toughness testing were performed on load line displacement CT specimens and extracted in the T-L orientation. The specimen thicknesses of X52 HRR and L360 NB specimens was 10 mm and 6 mm for the N80 Q. Side grooves were added on the toughness specimens, with depth equal to 5% of the specimen thickness on each side.

3.1.3.2 Fatigue pre-cracking

Fatigue pre-cracking was propagated from the starter notch by cyclic loading in a MTS servo-hydraulic machine following ASTM E647 procedures [2]. It was performed in air with a load cycle frequency f = 20 Hz and a load ratio R = 0.1. Propagation length from the starter notch was 3 mm (a_0 = 23 mm), corresponding to a_0/W = 0.575. The final K were : K_{final} = 20 MPa.m$^{0.5}$ for the fracture toughness specimens and K_{final} = 10 MPa.m$^{0.5}$ for the FCG specimens. After the test, specimens were immersed in liquid N_2 and open, allowing for measurements of fatigue pre-crack and final crack length by the nine-points method according to the ASTM E1820 [16], which were used for the validation and correction of the curves.

3.1.3.3 Fracture toughness test method

Fracture toughness testing was performed following the ISO12135:2002, CTOD method. The clip-on displacement (COD) has a maximum opening displacement of 3 mm, and all the tests were stopped once this limit was reached. The displacement rate used was 0.025mm.s^{-1}.

3.1.3.4 Fatigue crack growth test method

The FCGR test measures the crack propagation rate, da/dn, in a fatigue pre-cracked specimen, according to the stress intensity factor amplitude at the crack tip, ΔK. Testing was performed with R = 0.1 and f = 1 Hz, in environment.

3.2 Results

3.2.1 Fatigue crack growth results

Figure 2 presents the da/dn vs ΔK relationship obtained for the L360 NB and N80 Q steels, in NG and NG+H_2 mixtures saturated with water vapour. In Figure 2a, data obtained on the X52 HRR line pipe steel in NG+H_2 dry mixtures were added. The ΔK range investigated for the L360 NB was from 17 MPa.m$^{0.5}$ to 36 MPa.m$^{0.5}$. In this range, data measured in NG+H_2O presented a dispersion, which was not the case for the curves obtained in NG+25%H_2+H_2O that overlapped. For ΔK > 20 MPa.m$^{0.5}$, both da/dn vs. ΔK relationship in NG+25%H_2+H_2O and NG+H_2O increased with similar slope. However, crack growth rates in NG+25%H_2+H_2O were enhanced by a factor close to seven, compare to the rates in NG+H_2O. At lower ΔK (ΔK<20 MPa.m$^{0.5}$), the data in NG+25%H_2+H_2O presented a steep decrease of crack growth rate. X52 HRR data were obtained in NG, NG+2%H_2, NG+25%H_2 and 100%H_2 dry environments for a ΔK range running from 14 MPa.m$^{0.5}$ to 36 MPa.m$^{0.5}$. Data measured in NG+2%H_2, NG+25%H_2 and 100%H_2 almost overlapped for ΔK>20 MP.m$^{0.5}$. As ΔK decreased, crack growth rates decrease with a steeper slope in NG+2%H_2 than NG+25%H_2. The onset of this deceleration decreased towards lower ΔK with the increase of the hydrogen content in the gas mixture: in NG+2%H_2 this onset was observed at ΔK = 19 MPa.m$^{0.5}$ and at ΔK = 17 MPa.m$^{0.5}$ in NG+25%H_2. The ΔK curve in NG+2%H_2 reached the one in air at $\Delta K_{th,H2}$ = 15MPa.m$^{0.5}$. In 100% H_2 this steeper decrease was not observed for the ΔK range investigated, hence, in the conditions evaluated $\Delta K_{th,H2}$ is lower than 14 MPa.m$^{0.5}$. Data in NG and NG+H_2O for the X52 HRR and L360 NB respectively overlapped. The da/dn vs. ΔK relationships for the L360 NB and X52 HRR in hydrogen environments are similar for ΔK>20MPa.m$^{0.5}$. As ΔK decreases, crack growth rates of L360NB in NG+25%H_2+H_2O overlapped with data of X52 HRR in NG+2%H_2.

L360 NB specimens tested in NG+H_2O and NG+25%H_2+H_2O presented transgranular cracking and striations. Striations spacing was measured and found to be close to 1 µm, which corresponds to the crack growth measured at this ΔK (1 x 10^{-3} mm/cycle at ΔK = 24MPa.m$^{0.5}$).

Figure 2b presents the da/dn vs. ΔK relationship for the N80 Q measured in NG+H_2O and NG+25%H_2+H_2O. The results were duplicated; they highlighted a strong overlap for both environments respectively. Crack growth rates in hydrogen mixture saturated with water vapour was enhanced by a factor 5 compared to the crack growth rate in NG+H_2O. In the investigated ΔK range, the steep decrease of da/dn with ΔK was not observed for the ΔK range investigated; hence, in the conditions evaluated $\Delta K_{th,H2}$ is lower than 17 MPa.m$^{0.5}$.

At low ΔK (i.e. 20 MPa.m$^{0.5}$) the specimen tested in NG+H_2O presented facets characteristic of intergranular cracking. It can be assumed that the grain observed were prior austenite grains. As

ΔK increases, the fracture surface features changed to transgranular. In NG+25%H_2+H_2O, no intergranular features were observed; the fracture mode was entirely transgranular without the presence of brittle facets characteristic of hydrogen embrittlement.

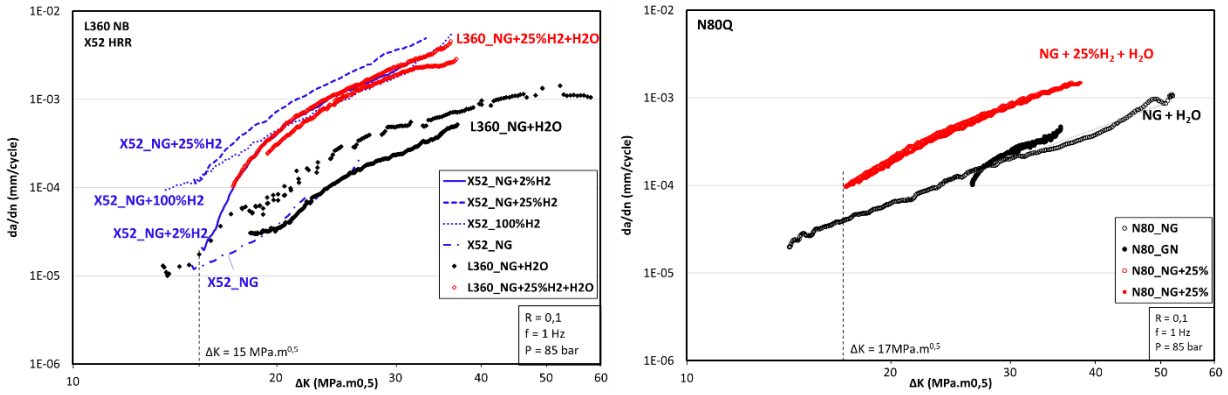

a) b)

Figure 2: FCG curves for the a) L360, X52 HRR and b) N80 Q. The results for the X52 HRR were obtained in GN, NG+2%H_2, NG+25%H_2 and 100%H_2 and in NG and NG+25%H_2 saturated in water vapour for the L360NB and N80 Q.

3.2.2 Fracture toughness results

Fracture toughness results of the L360 NB and N80 Q steels were measured in NG+H_2O, NG+25%H_2, NG+H_2S, NG+25%H_2+H_2S saturated with water vapour, with a P_{tot} = 85 bar at RT. A specimen of each material was also tested in NG+25%H_2 in dry environment and results on a X52 HRR measured in NG, NG+2%H_2, NG+25%H_2 were added for comparison. It is important to note that the L360NB and N80Q specimens tested in the presence of NG+H_2S+H_2O exhibited a dark layer deposit on both sides and this deposit was attenuated for the specimen tested in NG+25%H_2+H_2S+H_2O. Figure 3 presents the normalised load versus the crack opening displacement (COD) for each condition.

For the L360 NB, the normalised loads (Figure 3a) obtained in the presence of hydrogen were lower than the one without. For this material, in the presence of water vapour, the loads measured continuously increased with the COD (up to 3 mm) in NG+H_2O and NG+H_2O+H_2S, sign of no (or low) crack propagation, which was confirmed by fractographic observations. In NG+25%H_2+H_2O the load of one of the two specimens tested reached a plateau at the very end of the test. In the presence of NG+25%H_2+H_2O+H_2S the normalised force decreased as the COD grew. The specimen tested in NG+25%H_2 in dry conditions have the lowest resistance curve and the longest crack propagation. This highlighting the protecting role of water vapour toward HE, even in the presence of H_2S. Toughness results of the X52 HRR (blue continuous and dotted lines on Figure 3a were in the same load range than the ones of the L360 NB, however, they presented a contrasting behaviour. All the curves measured, with and without the presence of hydrogen, reached a maximum normalised force value and decreased. Hence, despite similar composition the X52 HRR had a lower toughness than the L360 NB in NG environment. This could be explained by its anterior manufacturing date and hence, a not as clean microstructure than the one of the L360, including the presence of inclusions. Toughness resistance of the X52 HRR decreased with the addition of

an increasing content of hydrogen and in the presence of hydrogen in dry environment, the resistance of the X52 HRR seems to be higher than the one of the L360 NB.

CTOD values are presented in Figure 4. In the case of the L360 NB, most of the curves F vs COD from which the CTOD values were extracted do not present a decrease and hence, the CTOD was calculated on the maximum load reached at the end of the test. For this reason, the given value (pointed with arrows on the graph) represents the minimum value that the CTOD could be in the tested conditions.

CTOD values confirmed the observations made on the graphs. The strong difference between the toughness properties of the L360 NB and X52 HRR steels in NG was highlighted with a CTOD medium value superior to 0,67 for the L360 NB and close to 0,3 mm for the X52 HRR. The loss of toughness, in NG+25%H_2 for the X52 HRR is close to 50%, while it seems to be none for the L360 NB in NG+25%H_2 saturated with water vapour. In NG+25%H_2+H_2O+H_2S the CTOD value for the L360 NB decreased compared to the one in NG+H_2O. Further, the CTOD value obtained in NG+25%H_2 dry was the lowest of the L360 NB CTOD values obtained and similar to the ones of the X52 HRR tested in NG+25%H_2 and 100%H_2.

For the N80 Q (Figure 3b), a similar trend was observed for the specimens tested without H_2S in the presence of H_2O (NG+H_2O and NG+25%H_2+H_2O), while in the presence of H_2S, the curves (NG+H_2S+H_2O and NG+25%H_2+H_2S+H_2O) were slightly lower. However, in dry environment: NG+25%H_2 the measured load vs COD was the lowest. This alloy presented a significantly different behaviour than the L360 NB in water vapour environment. A maximum normalised force value was achieved within the COD range in each condition. The CTOD measurements highlighted the lower resistance of the N80 Q compare to the L360, but this resistance in wet environment did not seem to be much affected by the presence of hydrogen and H_2S.

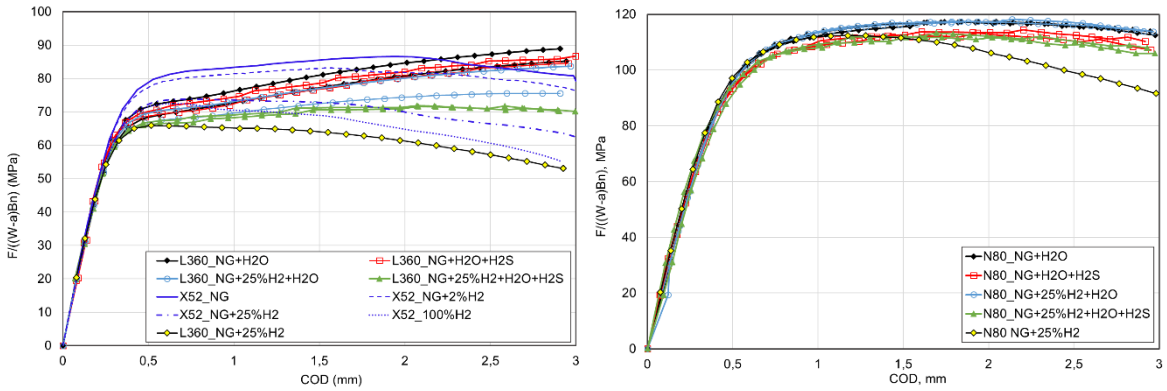

a) b)

Figure 3: Normalised force vs COD measured for the a) X52 HRR and L360 NB and b) N80 Q at P_{tot} = 85 bar and RT. The N80 Q and L360 NB were tested in NG, NG+25%H_2, NG+H_2S, NG+25%H_2+H_2S saturated with water vapour and NG+25%H_2 in dry environment. The X52 HRR was tested in NG, NG+2%H_2, NG+25%H_2.

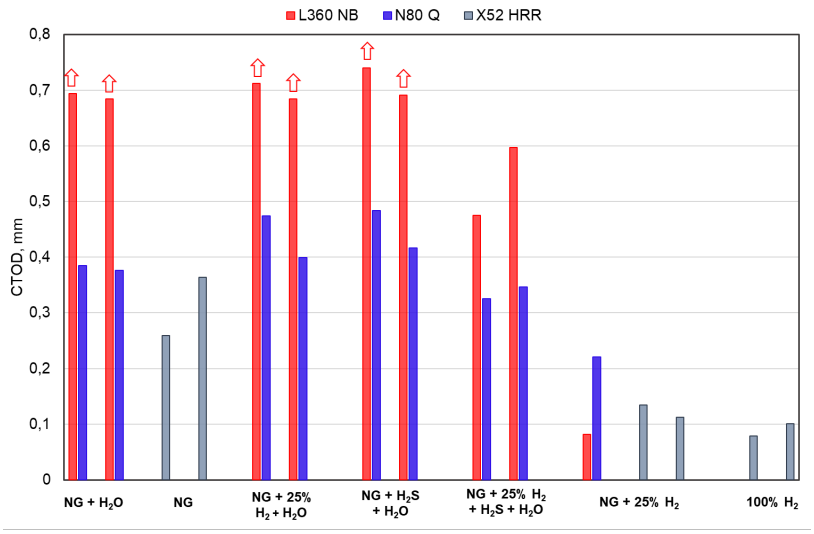

Figure 4: CTOD results extracted from the toughness results for the three alloys in their respective tested environments, P_{tot} = 85 bar and RT. The arrows represents the minimum value that the CTOD could be in the tested conditions.

3.3 Discussion

3.3.1 Influence of water vapour

In neutral environment, a higher proportion of micro-voids coalescence triggered by inclusions was observed on the fracture surface of the X52 HRR compared to the L360 NB. However, in NG+25%H_2 in dry environment, the L360 NB presented a slightly lower toughness than the X52 HRR. Hence, as soon as hydrogen is present modern and vintage steels have a similar behaviour. The inclusions lose their detrimental effect under hydrogen. This is consistent with the results presented by Ronevich et al. work [17]. These authors addressed vintage and modern pipeline steels in air and in hydrogen. They observed that the reduced inclusion content in modern steels improved the fracture toughness in neutral gas but has low effect in hydrogen.

The X52 HRR tested in dry NG+25%H_2 and the L360 NB tested in wet NG+25%H_2 presented similar FCGR for $\Delta K > 20 MPa.m^{0.5}$. However, the onset of the acceleration stage was shifted toward higher ΔK in wet environment. Similar observation was made by Somerday et al. [18] with oxygen: as oxygen content in hydrogen gas increased, the onset of acceleration stage was shifted toward higher ΔK. Above this ΔK threshold, the FCGR reached in 100%H_2 and in H_2+O_2 (content < 1000 ppmv) were similar. Oxygen creates a passive layer at the metal surface, which delays hydrogen entry in the material. The passive layer coverage competes with the bare surfaces that are created as the crack propagates: once a critical fatigue crack growth rate is reached, the bare surfaces created as the crack advances cannot be entirely covered by the passive layer, leaving new surfaces unprotected toward hydrogen entry. A similar mechanism with water vapour can be applied to the present study, with a competitive adsorption at the metal surface between H_2O and H_2.

The N80 Q presented an increasing FCGR in NG+25%H_2+H_2O compare to that in NG+H_2O. However, fracture toughness properties were not reduced in hydrogen wet environments. In a similar manner, fracture toughness results for the L360 NB tested in NG+25%H_2+H_2O presented a

very low loss of toughness compare to the test in NG+25%H_2 and for X52 HRR in NG+25%H_2. Hence, water vapour inhibits hydrogen embrittlement more efficiently during a fracture toughness test than a FCG test. Somerday et al. [18] and Wei [19] investigated the influence of R ratio on the shift of the onset of accelerated FCGR in the presence of oxygen content in hydrogen environment. They observed that for higher load ratio, the accelerating effect of hydrogen on FCGR could be entirely removed. From this observation, they were able to conclude that oxygen adsorption at the crack tip was not the limiting factor for passivation but mass transport to the crack tip was. During a fracture toughness test, there is no cycle loading and the CTOD is high compare to FCG testing conditions due to higher K. Thus, H_2O is always readily available for crack passivation. Hence, the limiting factor in FCGR for passivation, mass transport of water vapour at the crack tip, is not present in the case of a FT test. This explains the stronger inhibition of HE by water vapour on FT than on FCG tests.

3.3.2 Synergy in presence of $H_2 + H_2S + H_2O$

The fracture toughness properties of L360 NB have shown that hydrogen embrittlement susceptibility of this alloy presents the following trends: (NG+25%H_2+H_2O and NG+ H_2S+H_2O) < NG+25%H_2+H_2S+H_2O < NG+25%H_2. The highest susceptibility in dry environment compare to wet environment was addressed above. The highest susceptibility to HE in the presence of some H_2S (27 ppmv) and water vapour witnessed a synergistic influence of H_2, H_2S and H_2O. The hot melt extraction results did not highlight any significant effect of H_2S on H content. Hence, a catalytic effect of gaseous H_2S on H ingress in the metal is probably not the acting mechanism.
In aqueous environments, the combination of stress, H_2 and H_2S may results in catastrophic failures as a result of sulphide stress cracking (SSC). Only few articles have discussed the influence of gaseous hydrogen in presence of low amount of H_2S, but a common agreement on the fact that H_2S increased HE susceptibility emerged. Nelson et al.[14] observed the accelerated crack growth of a SAE 1020 steel in presence of 0.8 bar of H_2 mixed with 0.06 bar of H_2S, compared to that in 0.9 bar of H_2. Fukuyama et al. [13] made similar observation on FCG results of a CrMo steel. They concluded that H_2S was a strong promoter of hydrogen embrittlement by the following mechanism: H_2S reduces at the metal surface, freeing a nascent hydrogen enabled to generate HE. Conclusions of Kerns et al. [20] investigation were similar. They performed toughness test under constant load in presence of 0.13 bar of H_2 with H_2S concentration from 0.01%mol to 0.1%mol (100 ppmv to 1000 ppmv). They observed a higher degradation of toughness properties in presence of H_2S with an increase of the crack growth velocity of 16% from the addition of 0.02%mol H_2S. From this observation, they concluded that H_2S acts in the same manner than in aqueous environment by accelerating hydrogen entry in the material.

However, there are no results in the literature concerning the effect of a combined H_2, H_2O and few ppmv of H_2S in gaseous environment. Our results outline a synergy between these gases; this could be explained by capillary condensation at the crack tip and high H_2S solubility in liquid water, as described below.

Johnson and Willner work [21] on the influence of water vapour environment on a H11 Cr-based steel have observed similar fatigue crack growth conditions at 60% of relative humidity (RH) in water vapour and in aqueous environment. It has often been reported that condensation may occur on specific locations (edges, rust particles) at such relative humidity. From this observation, the authors concluded that capillary condensation occurred at the crack tip, creating locally, and similar crack growth conditions than in aqueous media. Similar statement was also made by Hutin

[22] on a AISI 4130 at RH 40%. Indeed, the equilibrium vapour pressure at vapour-solid interface is a function of interface curvature [5]. The low radius at the crack tip will favour condensation of water especially for a saturated gas.

The environment of the present study was saturated by water vapour. Furthermore, the dark deposit observed on the specimens sides tested in the presence of H_2S is thought to be ferrous sulphides, formed in aqueous environment. Thus, after gaseous diffusion of water vapour towards the crack tip, condensation may occur due to the small curvature radius. On one hand, the presence of a water drop at the crack tip could explain the delay in hydrogen ingress in the N80 Q and L360 NB and hence the inhibiting effect of H_2O. On the other hand, in NG+25%H_2+H_2S+H_2O, H_2S dissolved in the water drop at the crack tip, creating locally a "sour" environment, promoting HE. Thus, it is proposed that capillarity condensation is the acting mechanism leading to the synergistic and detrimental effect observed in H_2S+H_2 in a wet environment.

4 Conclusions & Overall Recommendations

This work investigated FCG and fracture toughness properties of a tempered martensite N80 Q steel, and a ferrite-perlite L360 NB C-Mn steel in NG, NG + H_2S, NG + 25%H_2 and NG + 25%H_2 + H_2S saturated in water vapour at 8.5 MPa total pressure and room temperature. The main conclusions are the following:

- Despite wet environment, the FCGR for both materials (N80Q and L360 NB), are enhanced by a factor close to 5 in the presence of NG+25%H_2+H_2O in the Paris regime. This highlights the low HE mitigation effect of H_2O for this mechanical loading mode.
- By contrast, the onset of FCGR enhancement by hydrogen ($\Delta K_{th,H2}$) is shifted toward higher ΔK for L360 NB. At low ΔK, H_2O seems to be a partial inhibitor for this alloy. This was explained by the competition between the crack advance and H_2O coverage.
- In contrast with the FCG results, FT results featured that H_2O inhibits HE effect for both alloys. An attempt to explain this distinction was that: in the case of FCG, the limiting factor for H_2O inhibition is its mass transport at the crack tip induced by cyclic loading which, due to fundamentally different loading mode is absent in the case of FT.
- The effect of low amount of H_2S in wet H_2 has been addressed on fracture toughness properties. L360 NB behaviour is slightly degraded by the combination of H_2+H_2S+H_2O, compared to the H_2+H_2O and H_2S+H_2O. A synergetic effect between these three gases is observed. This synergy can be explained by a capillarity condensation mechanism, creating a sour environment at the crack tip.

5 References

[1] U. Weichenhain, 'Hydrogen Valleys. Insights into the emerging hydrogen economies around the world', Mar. 2021.

[2] J. Andersson and S. Grönkvist, 'Large-scale storage of hydrogen', *International Journal of Hydrogen Energy*, vol. 44, no. 23, pp. 11901–11919, May 2019.

[3] A. M. Elberry, J. Thakur, A. Santasalo-Aarnio, and M. Larmi, 'Large-scale compressed hydrogen

storage as part of renewable electricity storage systems', *International Journal of Hydrogen Energy*, vol. 46, no. 29, pp. 15671–15690, Apr. 2021.

[4] IEA, 'The future of hydrogen - Analysis', *Technology*, 2019, [Online]. Available: https://www.iea.org/reports/the-futureof-hydrogen.

[5] S. S. Kalati, N. Pour Khiabani, S. Ayatollahi, H. Mahani, D. Zivar, and M. A. Esmaeilbeig, 'Molecular dynamics simulation of hydrogen diffusion into brine: Implications for underground hydrogen storage', *International Journal of Hydrogen Energy*, vol. 53, pp. 17–28, Jan. 2024.

[6] A. Amid, D. Mignard, and M. Wilkinson, 'Seasonal storage of hydrogen in a depleted natural gas reservoir', *International Journal of Hydrogen Energy*, vol. 41, no. 12, pp. 5549–5558, Apr. 2016.

[7] A. Ozarslan, 'Large-scale hydrogen energy storage in salt caverns', *International Journal of Hydrogen Energy*, vol. 37, no. 19, pp. 14265–14277, Oct. 2012, doi: 10.1016/j.ijhydene.2012.07.111.

[8] D. Zivar, S. Kumar, and J. Foroozesh, 'Underground hydrogen storage: A comprehensive review', *International Journal of Hydrogen Energy*, vol. 46, no. 45, pp. 23436–23462, Jul. 2021.

[9] S. R. Thiyagarajan, H. Emadi, A. Hussain, P. Patange, and M. Watson, 'A comprehensive review of the mechanisms and efficiency of underground hydrogen storage', *Journal of Energy Storage*, vol. 51, p. 104490, Jul. 2022.

[10] M. Dadfarnia, A. Nagao, S. Wang, M. L. Martin, B. P. Somerday, and P. Sofronis, 'Recent advances on hydrogen embrittlement of structural materials', *International Journal of Fracture*, vol. 196, no. 1–2, pp. 223–243, Nov. 2015.

[11] K.-O. Bae, H.-S. Shin, and U.-B. Baek, 'Quantitative evaluation of hydrogen embrittlement susceptibility in various steels for energy use using an in-situ small punch test', *International Journal of Hydrogen Energy*, vol. 46, no. 38, pp. 20107–20118, Jun. 2021.

[12] C. San Marchi and J. A. Ronevich, 'Fatigue and Fracture of Pipeline Steels in High-Pressure Hydrogen Gas', in *Volume 4B: Materials and Fabrication*, Las Vegas, Nevada, USA: American Society of Mechanical Engineers, Jul. 2022, p. V04BT06A034.

[13] S. Fukuyama and K. Yokogawa, 'Prevention of hydrogen environmental assisted crack growth of 2.25Cr-1Mo steel by gaseous inhibitors', *Pressure Vessel Technology*, pp. 914–923, 1990.

[14] H. G. Nelson, 'Hydrogen-induced slow crack growth of a plan carbon pipeline steel under conditions of cyclic loading', Moffett Field, California 94035: The Metallurgical Society of AIME, 1976, pp. 602–611.

[15] K. Yokogawa, S. Fukuyama, G. Han, and J. He, 'Hydrogen environment embrittlement of materials for hydrogen energy service', *World Energy Network*, 1996.

[16] 'ASTM E1820-18a_Standard Test Method for Measurement of Fracture Toughness', ASTM International, Standard, 2018.

[17] J. Ronevich, R. Shrestha, and C. S. Marchi, 'Misconceptions of Hydrogen Degradation of Pipeline Steels in Existing Natural Gas Infrastructure', p. 13, Oct. 2022.

[18] B. P. Somerday, P. Sofronis, K. A. Nibur, C. San Marchi, and R. Kirchheim, 'Elucidating the variables affecting accelerated fatigue crack growth of steels in hydrogen gas with low oxygen concentrations', *Acta Materialia*, vol. 61, no. 16, pp. 6153–6170, Sep. 2013.

[19] T.-H. Shih and R. P. Wei, 'The effects of load ratio on environmentally assisted fatigue crack growth', *Engineering Fracture Mechanics*, vol. 18, no. 4, pp. 827–837, Jan. 1983.

[20] G. E. Kerns and R. W. Staehle, 'Slow crack growth in hydrogen and hydrogen sulfide gas environments', *Scripta Metallurgica*, vol. 6, pp. 631–634, 1972.

[21] H. H. Johnson and A. M. Willner, 'Moisture and stable crack growth in a high strength steel', *Applied Mat Research*, pp. 34–40, 1965.

[22] J.-P. Hutin, 'Sub-critical crack growth in AISI 4340 steel in water and water vapor', Degree of Master of Science in Applied Mechanics, Lehigh University, 1975.